Linear Approximation of Sensitivity Curve Calibration

Dietrich Paulus[1] Joachim Hornegger[2] László Csink[3]

Universität Koblenz-Landau	Siemens Medical Solutions	Budapest Polytechnic
Computational Visualistics	Inc.	John von Neumann Faculty of
Universitätsstr. 1	AXE Siemensstr. 1	Informatics
56070 Koblenz	91301 Forchheim	H-1300 Budapest
paulus@uni-koblenz.de	joachim@hornegger.de	csink@nik.bmf.hu

Abstract

Calibration of color cameras requires that a calibration pattern is recorded and color sensitivity curves are estimated from the recorded data. Very often, these curves are sampled at discrete wavelength, so that the calibration problem can be written as a system of linear equations. The solution of the – usually overdetermined – problem is subject to a constrained optimization problem, as these curves need to have a certain shape. In this article we apply different methods to incorporate constraints into the estimation problem while still keeping the problem linear.

1   Introduction

Color cameras have sensors that have an unknown sensitivity functions. The sensitivity of typical CCD chips for red, green, and blue varies over the range of wavelenghts λ. The sensors may even vary amongst the same type as the sensitivity curves depend on the parameters of the production. Therefore, color calibration of a camera requires the estimation of color sensitivity curves. If the sensitivity functions are known, color pixels can be re-mapped to values of a standard observer. Accurate color measurements require such a mapping. In many cases, accurate color values might increase results of image analysis.

The goal is to compute these parameters automatically. Usually, this is done under known illumination with a color checker and spectrometric measurements. Several unknown parameters influence the image generation process. It is usually assumed that the spectral energy distribution of the light source $E(\lambda)$ is known. A calibration pattern[1] with known reflectivity $S(\boldsymbol{x}, \lambda)$ at spatial position $\boldsymbol{x}$ is recorded and color pixel vectors corresponding to the position $\boldsymbol{x}$ will be used to set up an equation system for the unknonw influence of the sensor (Figure 1).

In the following we describe mathematical models for this process. As the computation of the unknowns is an overdetermined system with constraints, [1] uses non-linear optimization to

---

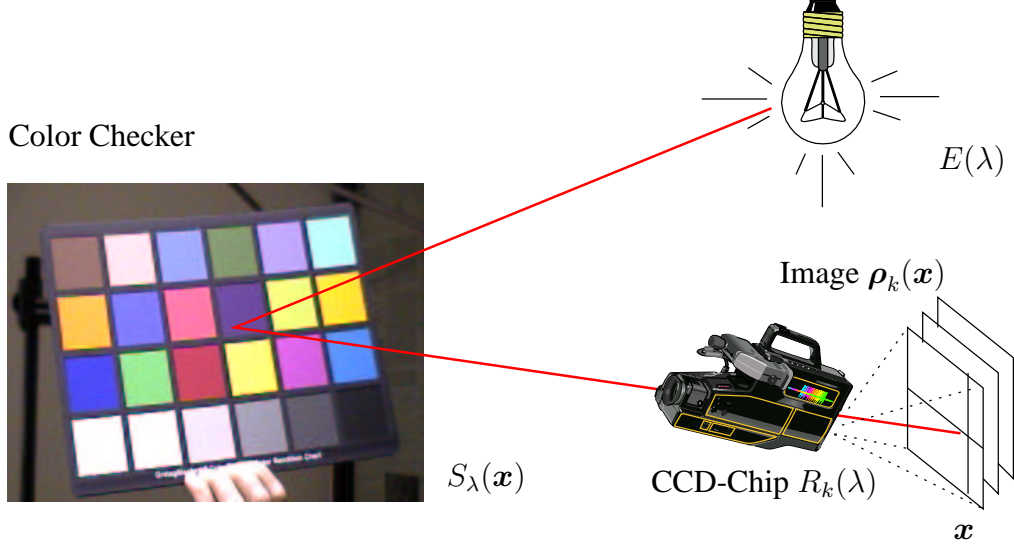[1]For example the Gretag McBeth ColorChecker, shown on the left in Figure 1

Figure 1: Sensor, reflectivity, and measurements

compute the sensitivity functions. [2] reports on several approaches and uses Fourier basis functions to approximate the sensitivity curves. In the following we will derive a linear approximation of calibration parameters.

2 Device Sensitivity Model

The K sensors per pixel, typically red, green, and blue for a color camera, have spectral sensitivity curves $R_k(\lambda), (k = 1, \ldots, K)$. Any sensor k thereby records light intensity at position x using the following energy distribution (cmp. [6, Sect.. 2.2.3]):

$$\rho_k(\boldsymbol{x}) = \int_0^\infty E(\lambda) \cdot S(\boldsymbol{x}, \lambda) \cdot R_k(\lambda) \, d\lambda \tag{1}$$

As noted in [1], the discrete version of (1) is often written as a sum of $L = 31$ samples

$$\rho_k(\boldsymbol{x}) = \sum_{\lambda=1}^L E_\lambda \cdot S_\lambda(\boldsymbol{x}) \cdot R_{k,\lambda} \cdot \Delta\lambda \quad . \tag{2}$$

The vector $\boldsymbol{E} = [E_\lambda]_{\lambda=1\ldots L}$ denotes discrete spectral energy distribution for light, $\boldsymbol{S}(\boldsymbol{x}) = [S_\lambda(\boldsymbol{x})]_{\lambda=1\ldots L}$ denotes discrete reflectance at position $\boldsymbol{x}$, and the matrix $\boldsymbol{R} = (R_{k,\lambda})_{k=1,\ldots,K,\lambda=1\ldots L}$ denotes the discrete spectral sensitivity curves of the sensors. Using $\Delta\lambda = 10\texttt{nm}$, the whole visible range of light can be covered. In the following we discard the scalar constant $\Delta\lambda$ in the equations for simplicity. The relation of the various variables is shown in Figure 1.

We now arrange (2) into a matrix equation, as we re-write matrix $\boldsymbol{R}$ as a vector

$$\boldsymbol{r} = (R_{1,1} \ldots R_{1,L}, R_{2,1} \ldots R_{2,L}, \ldots R_{K,1} \ldots R_{K,L})$$

and define a $(KN \times LK)$ - matrix $\boldsymbol{C}$ consisting of sensor responses measured at N points of either zeros or products $E_\lambda \cdot S_\lambda$ to get

$$\boldsymbol{\rho} = \boldsymbol{C}\boldsymbol{r} \quad .\tag{3}$$

More specifically, with $K = 3$ this is

$$
\begin{pmatrix}
\rho_{1,\text{red}} \\
\rho_{1,\text{green}} \\
\rho_{1,\text{blue}} \\
\cdots \\
\rho_{N,\text{red}} \\
\rho_{N,\text{green}} \\
\rho_{N,\text{blue}}
\end{pmatrix}
= \boldsymbol{C}
\begin{pmatrix}
R_{\text{red},1} \\
R_{\text{red},2} \\
\vdots \\
R_{\text{red},L} \\
\cdots \\
R_{\text{blue},1} \\
R_{\text{blue},2} \\
\vdots \\
r_{\text{blue},L}
\end{pmatrix}
\tag{4}
$$

and

$$
\boldsymbol{C} =
\begin{pmatrix}
E_1 S_1^{(1)} & \cdots & E_L S_L^{(1)} & 0 & \cdots & 0 & 0 & \cdots & 0 \\
0 & \cdots & 0 & E_1 S_1^{(1)} & \cdots & E_L S_L^{(1)} & 0 & \cdots & 0 \\
0 & \cdots & 0 & 0 & \cdots & 0 & E_1 S_1^{(1)} & \cdots & E_L S_L^{(1)} \\
\vdots & \vdots & \vdots & \vdots & \vdots & \vdots & \vdots & \vdots & \vdots \\
E_1 S_1^{(N)} & \cdots & E_L S_L^{(N)} & 0 & \cdots & 0 & 0 & \cdots & 0 \\
0 & \cdots & 0 & E_1 S_1^{(N)} & \cdots & E_L S_L^{(N)} & 0 & \cdots & 0 \\
0 & \cdots & 0 & 0 & \cdots & 0 & E_1 S_1^{(N)} & \cdots & E_L S_L^{(N)}
\end{pmatrix}
\tag{5}
$$

Assuming standard illumination, i.e., E_λ is known, and knowledge on the reflectivity and surface of the object, i.e., S_λ are known, we can measure $\boldsymbol{\rho}$ and compute the unknown vector $\boldsymbol{r}$. Usually, standard lighting techniques are used and a color checker pattern (e.g., the Gretag McBeth color chart) is placed in front of the camera. Correspondence of known colors and their position in the image accounts for the positions $\boldsymbol{x}$ in (2) and for the N measurement points in (4). In order to get a solution of the set of linear equations, the number of measurements N must be greater than L.

An empirical result states that for $K = 3$ the matrix $\boldsymbol{C}$ has only rank 6 to 8 [4, 5]; in addition to the linear equation (3) further constraints are used to obtain a resonable result by regularization [1]:

1. sensor positivity:
   $R_{k,\lambda} > 0$ where $k \in \{1, \ldots, K\}, \lambda \in \{1, \ldots, L\}$

2. sensor smoothness:
   $|R_{k,\lambda} - R_{k,\lambda+1}| < T$ for some threshold T and $\lambda \in \{1, \ldots, L-1\}$

3. unimodality:
   $\forall k \exists \kappa : R_{k,\lambda} < R_{k,\lambda+1}$ for $\lambda \leq \kappa$ and $R_{k,\lambda} > R_{k,\lambda+1}$ for $\lambda > \kappa$

4. bounded prediction error:
   $|\rho_i - \sum_{j=1}^{L} C_{i,j} \cdot r_j| \leq \epsilon$ for $i \in \{1, \ldots, N\}$.

   To obtain a subset of these constraints, several optimization techniques have been proposed, such as linear programming or quadratic programming.

3   Simultaneous Optimization

In the following we derive an optimization of the criteria 1–4 where some of the criteria have to be replaced by slightly weaker constraints. Instead of iterative optimization techniques weaker constraints lead to a linear problem that will be solved using SVD. Inequalities are replaced by a single objective function which has to be minimized finally. For each of the criteria we introduce a term in the objective function.

Clearly, the criterion 4 is described by

$$||\boldsymbol{Cr} - \boldsymbol{\rho}||^2 \to \min \quad . \tag{6}$$

The constraint for sensor smoothness in constraint 2 requires that two adjacent coefficients $R_{k,\lambda}$, $R_{k,\lambda+1}$ differ only up to a threshold. This constraint is slightly weakened as we use

$$\sum_{k=1}^{K} \sum_{\lambda=1}^{L-1} \left(R_{k,\lambda} - R_{k,\lambda+1} \right)^2 \to \min \quad . \tag{7}$$

Since the squared difference is used instead of the norm $|R_{k,\lambda} - R_{k,\lambda+1}|$ as in constraint 2, large differences are more penalized and imply a bias. We define a $L \times L$ matrix[2]

$$\tilde{\boldsymbol{D}} = \begin{pmatrix} 1 & -1 & 0 & 0 & \ldots & \ldots & 0 \\ -1 & 2 & -1 & 0 & \ldots & \ldots & 0 \\ 0 & -1 & 2 & -1 & 0 & \ldots & 0 \\ \ldots & & & & & & \\ 0 & \ldots & 0 & -1 & 2 & -1 & 0 \\ 0 & \ldots & \ldots & 0 & -1 & 2 & -1 \\ 0 & \ldots & \ldots & \ldots & 0 & -1 & 1 \end{pmatrix}$$

and another $K \cdot L \times K \cdot L$ matrix

$$\boldsymbol{D} = \begin{pmatrix} \tilde{\boldsymbol{D}} & \boldsymbol{0} & \cdots & \boldsymbol{0} \\ \boldsymbol{0} & \tilde{\boldsymbol{D}} & \cdots & \boldsymbol{0} \\ \vdots & \vdots & \vdots & \vdots \\ \boldsymbol{0} & \boldsymbol{0} & \boldsymbol{0} & \tilde{\boldsymbol{D}} \end{pmatrix} \quad .$$

---

[2]This matrix can be also interpreted as a second derivative, as it is used in the constraints in [2].

Then, constraint 2 can be expressed as

$$\sum_{k=1}^{L} \sum_{\lambda=1}^{L-1} \left(r_{k,\lambda} - r_{k,\lambda+1} \right)^2 = \boldsymbol{r}^{\mathrm{T}} \boldsymbol{D} \boldsymbol{r} \rightarrow \min \quad . \tag{8}$$

The derivatives are

$$\frac{\partial}{\partial \boldsymbol{r}} \boldsymbol{r}^{\mathrm{T}} \boldsymbol{D} \boldsymbol{r} = 2 \cdot \boldsymbol{r}^{\mathrm{T}} \boldsymbol{D} \quad , \tag{9}$$

as $\boldsymbol{D}$ is symmetric. Combining (8) and (6) we get

$$f := ||\boldsymbol{C} \boldsymbol{r} - \boldsymbol{\rho}||^2 + \mu ||\boldsymbol{r}^{\mathrm{T}} \boldsymbol{D} \boldsymbol{r}|| \rightarrow \min \tag{10}$$

for a fixed $\mu > 0$. Computing the derivatives of (10) we get

$$\frac{\partial f}{\partial \boldsymbol{r}} = 2 \boldsymbol{r}^{\mathrm{T}} \boldsymbol{C}^{\mathrm{T}} \boldsymbol{C} - 2 \boldsymbol{\rho}^{\mathrm{T}} \boldsymbol{C} + 2 \mu \cdot \boldsymbol{r}^{\mathrm{T}} \boldsymbol{D} \tag{11}$$

which is a row vector of dimension $K \cdot L$. We set

$$\frac{\partial f}{\partial \boldsymbol{r}} = 0$$

and solve that for $\boldsymbol{r}$, as we will show in the following. Thus we get

$$\boldsymbol{r}^{\mathrm{T}} \left(\boldsymbol{C}^{\mathrm{T}} \boldsymbol{C} + \mu \cdot \boldsymbol{D} \right) = \boldsymbol{\rho}^{\mathrm{T}} \boldsymbol{C} \quad . \tag{12}$$

As $\left(\boldsymbol{C}^{\mathrm{T}} \boldsymbol{C} + \mu \cdot \boldsymbol{D} \right)$ is symmetric and positive definite, we get

$$\boldsymbol{r} = \left(\boldsymbol{C}^{\mathrm{T}} \boldsymbol{C} + \mu \cdot \boldsymbol{D} \right)^{-1} \boldsymbol{C}^{\mathrm{T}} \boldsymbol{\rho} \quad . \tag{13}$$

This regularization is similar, but not identical with the Tikhonov regularization used in [7].

We now turn to the constraint that rank $(\boldsymbol{C}) \leq 8$. To enforce this, we factorize $\boldsymbol{C} = \boldsymbol{U} \boldsymbol{\Sigma} \boldsymbol{V}^{\mathrm{T}}$ using singular value decomposition, i.e. $\boldsymbol{\Sigma}$ is the diagonal matrix containing the singular values σ_i of $\boldsymbol{C}$, $\boldsymbol{\Sigma} = \mathrm{diag} (\sigma_i)$ with $\sigma_i \geq \sigma_{i+1}$. It is well known from linear algebra that setting singular values to 0 in $\boldsymbol{\Sigma}$ yielding $\boldsymbol{\Sigma}'$ we can enforce the rank of $\boldsymbol{U} \boldsymbol{\Sigma}' \boldsymbol{V}^{\mathrm{T}}$. We introduce a matrix $\boldsymbol{P} = [P_{ij}]_{i,j=1...N}$ where $P_{ij} = 1$ for the first eight elements on the diagonal and 0 everywhere else; this matrix is used to generate $\boldsymbol{\Sigma}'$ as $\boldsymbol{\Sigma}' = \boldsymbol{P} \boldsymbol{\Sigma}$. We check $P_{9,9} = \sigma_9 > \theta$ for some small threshold θ; if this is not true, our measurement matrix $\boldsymbol{C}$ cannot be correct or it contains too much measurement noise. Integrating this into (13) gives the new combined equation

$$\boldsymbol{r} = \left(\boldsymbol{V} \boldsymbol{P} \boldsymbol{\Sigma}^2 \boldsymbol{V}^{\mathrm{T}} + \mu \cdot \boldsymbol{D} \right)^{-1} \boldsymbol{V} \boldsymbol{P} \boldsymbol{\Sigma} \boldsymbol{U}^{\mathrm{T}} \boldsymbol{\rho} \quad . \tag{14}$$

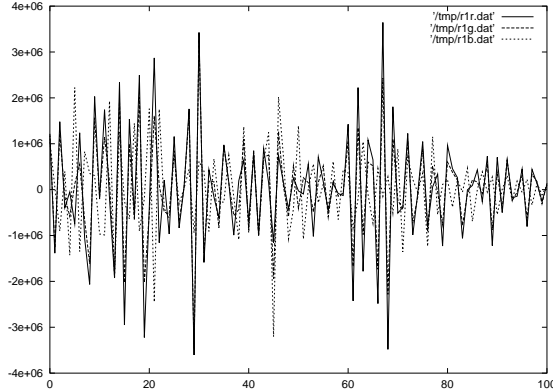We now need to check whether the positivity of the results is valid. If not, we discard the result.

Figure 2: Solution with $\mu = 0$, i.e. by pseudo inverse

4 Experiments

In [3], data are shown for $K = 3$ and $L = 101$.[3] We used these data for our experiments. As can be seen from Figure 2, regularization is required.

[2] used various basis functions such as a Fourier basis to approximate the sensitivity curves by a linear combination of these functions. Thereby unimodality of the sensitivity curves can be achieved. A solution of (15) without further constraints will yield a solution, that may have local maxima, but other than that is feasible (Figure 3).

It turned out in the experiments that enforcing the rank to 8 in (14) leads to a matrix with a very large condition number. The rank was thus enforced as in

$$r = \left(V \Sigma^2 V^{\mathrm{T}} + \mu \cdot D \right)^{-1} V P \Sigma U^{\mathrm{T}} \rho \tag{15}$$

which lead to mathematically more stable results, which where, however, not convincing, as can be seen in Figure 4.

Forcing the rank of C to 25 by (14) results in curves that are almost identical to those of the full rank C, which numerically is 303 (Figure 5, left). Thereby, many operations can be saved in the computation. Forcing it to 25 by (15) mostly preservers unimodality and positivity.

5 Conclusion

From the figures it is clear that the positivity constraint can be fulfilled automatically by the smoothness regularization, if $\mu < 0.01$. Unimodality is not obtained without additional constraints or tools. In practice, it can be enforced by clipping the curves to zero when they reach a local minimum. This is also possible, if $\mu > 0.01$ is chosen and negative values are computed for the three curves.

---

[3]The data are available on the internet in
`http://www.cs.berkeley.edu/~kobus/research/data/camera_calibration/index.html`.
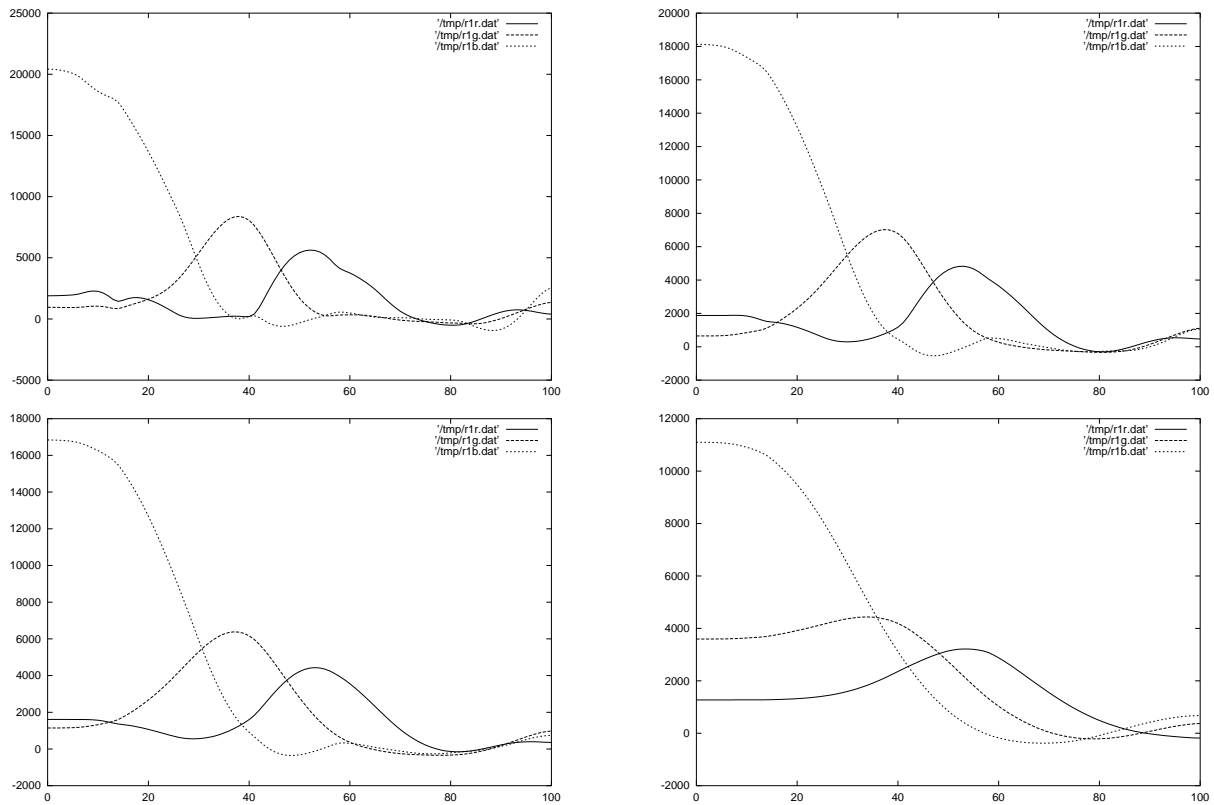
Figure 3: Solutions for $\mu = 0.001$, $\mu = 0.005$, $\mu = 0.01$, and $\mu = 0.1$

Acknowledgement

References

[1] A. Alsam and G. Finlayson. Recovering spectral sensitivities with uncertainty. In *Proceedings of the First international Conference CGIV*, pages 22–26, Poitiers, France, 2002.

[2] K. Barnard and B. Funt. Camera characterization for color research. *Color Research and Application*, 27(3):153–164, 2002.

[3] K. Barnard, L. Martin, B. Funt, and A. Coath. A data set for color research. *Color Research and Application*, 27(3):148–152, 2002.

[4] L.T. Maloney. Evaluation of linear models of surface spectral reflectance with small numbers of parameters. *J. Opt. Soc. Am. A*, 3:1673–1683, 1986.
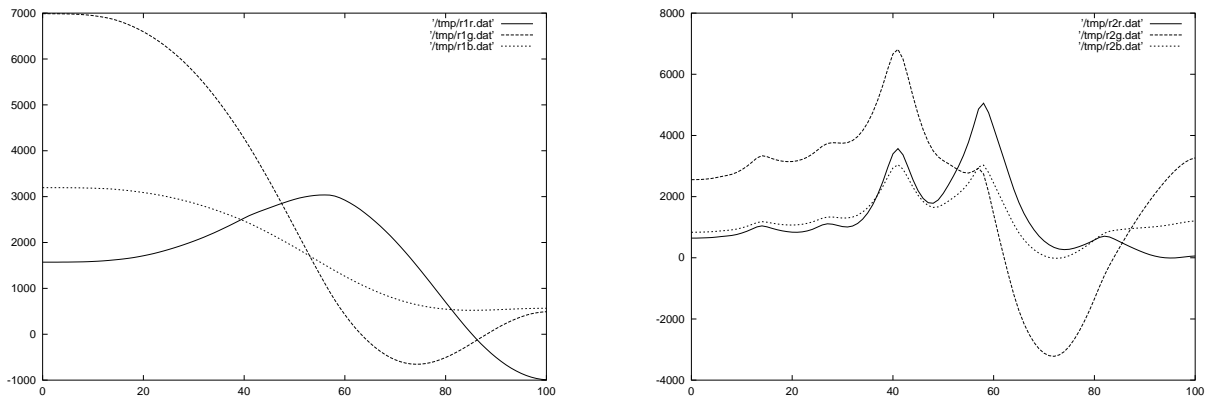
Figure 4: Solutions for $\mu = 0.001$ rank enforced to 8 by (14) (left), enforced to 8 by (15) (right)
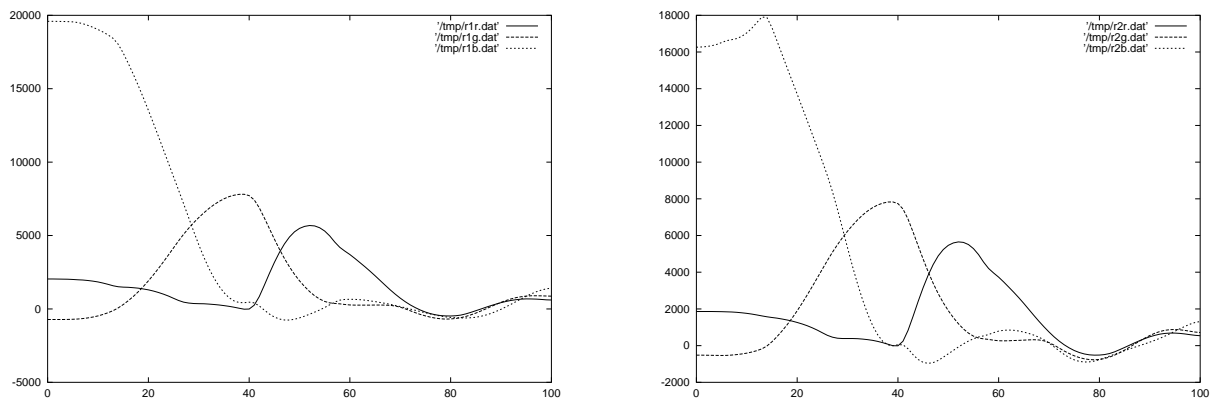

Figure 5: Solutions for $\mu = 0.001$ rank enforced to 25 by (14) (left), enforced to 25 by (15) (right)

[5] J. P. S. Parkkinen, J. Hallikanen, and T. Jaaskelainen. Characteristic spectra of munsell colors. *J. Opt. Soc. Am. A*, 6:318–322, 1989.

[6] D. Paulus. *Aktives Bildverstehen*. Der andere Verlag, Osnabrück, 2001. Habilitationsschrift in der Praktischen Informatik, Universität Erlangen-Nürnberg, Mai 2000.

[7] Piana and J.C. Brown. Optimal inversion of hard x-ray bremsstrahlung spectra. *Astron. Astrophys. Suppl.*, 132:291–299, 1998.